

Evaluation of surface roughness of anatomical structures models of the mandible made with additive techniques from selected polymeric materials (*Rapid communication*)

Paweł Turek^{1), *)} (ORCID ID: 0000-0002-5926-4815)

DOI: dx.doi.org/10.14314/polimery.2022.4.4

Abstract: The influence of polylactide (PLA), polycarbonate (PC), polyacrylic photo resins and polyamide 11 (PA11) on the surface roughness of anatomical models structures of the mandible made with additive techniques was investigated. Measurements of the model surfaces geometric structure were carried out using a 3D contact profilometer. Selected roughness parameters and three-dimensional visualization of the tested models surface roughness are presented.

Keywords: additive techniques, polymer materials, surface roughness, anatomical structure model, contact measurements.

Ocena chropowatości powierzchni modeli struktur anatomicznych żuchwy wykonanych technikami przyrostowymi z wybranych materiałów polimerowych

Streszczenie: Zbadano wpływ polilaktydu (PLA), poliwęglanu (PC), żywicy foto poliakrylowych i poliamidu 11 (PA11) na chropowatość powierzchni modeli struktur anatomicznych żuchwy wykonanych technikami przyrostowymi. Pomiary struktury geometrycznej powierzchni modeli przeprowadzono przy użyciu profilometru stykowego. Przedstawiono wybrane parametry chropowatości oraz trójwymiarowe wizualizacje chropowatości powierzchni badanych modeli.

Słowa kluczowe: techniki przyrostowe, materiały polimerowe, chropowatość powierzchni, model struktury anatomicznej, pomiary stykowe.

As it is known, additive manufacturing techniques consist in the layering and bonding of material to produce a physical model based on data from the Stereolithography (STL) file [1]. Various types of materials are used to print models. Currently, due to the continuous improvement of mechanical and functional properties, the scope of polymeric materials application is expanding in the additive process of shaping the products geometry [2, 3]. Depending on the technique used, polymeric materials can take a solid, liquid or semi-liquid form during printing. Currently, rapid prototyping techniques are used in many areas, including the aviation [4, 5] and automotive industries [4]. In recent years, polymeric materials and 3D printing are also very often used in medicine, e.g.: in the process of visualizing the geometry of anatomical structures [6,7] and in the process of making surgical templates and implants [8].

The mandible is the most specific area of the facial skeleton. It is the only movable bone that is subjected to multidirectional dynamic loads during the biting and chewing process. As a result of breaking the continuity of the mandible, there are: impaired airway patency, dysphagia, speech and chewing disorders as well as deformities of the lower part of the face [9]. In the event of such a situation, surgical templates or implants are most often used during the procedure to restore the geometric continuity of the mandible. Making a template or implant for surgery is not a simple task. This is especially true of the craniofacial area, which consists of bone tissues with a very complex geometry. Titanium alloys are still used in medicine as implantable materials. However, due to the continuous improvement of mechanical and functional properties, the scope of polymeric materials application in medicine is expanding. Each model used directly or indirectly during a surgical procedure must meet many conditions. They must meet all the requirements allowing direct or indirect contact with human tissue. Currently, the additive techniques of material extrusion (MEX) [10–12], material jetting (MJT) [13–15], powder bed fusion (PBF) [16, 17] and vat polymerization (VPP) [18] are most

¹⁾ Rzeszów University of Technology, Faculty of Mechanical Engineering and Aeronautics, Department of Manufacturing Techniques and Automation, al. Powstańców Warszawy 8, 35-959 Rzeszów, Poland.

*) Author for correspondence: pturek@prz.edu.pl

Table 1. Polymer materials characterization

Property	PLA	PC	AR1	AR2	AR3	PA11
Tensile strength, MPa	53	57	57	56	50	40
Elongation at break, %	6	4	4	4	20	18
Flexural strength, MPa	–	–	129	115	75	–
Notched Izod impact strength, J/m	16	86	–	–	–	8
Heat deflection temperature, °C	55	133	130	140	48	110

often used in the process of model production within the craniofacial area. In the case of these methods, mainly polymeric materials are used: polylactic acid (PLA) [11], polycarbonate (PC) [12], polyamide (PA) [16, 17] and photosensitive resins [13–15, 18].

The aspect of the surface layer technological assessment is also a key factor for models made with additive methods. Surface roughness plays a particularly important role in terms of the objects functionality. In the case of models used in the medical industry, it influences, among other things, the functional activity of cells in the immediate vicinity of the implant and modulates the osteoblasts adhesion. It also increases their enzymatic activity and determines the amount and type of proteins synthesized by it [19]. Due to the continuous increase in the use of anatomical structures printed models, surgical templates and implants made of polymeric materials, it is necessary to test the surface roughness of the obtained models constantly in order to adapt their surface layer to the conditions enabling their use in direct or indirect contact with human tissues.

In this study, the evaluation of surface roughness of anatomical structures models of the mandible made with additive techniques from polylactic acid (PLA), polycarbonate (PC), polyamide 11 (PA11) and photosensitive resins was investigated. These polymers are commonly used in processes, including making models of anatomi-

cal structures and surgical templates for planning surgical procedures in the craniofacial area [10–12, 16].

EXPERIMENTAL PART

Materials

Six types of polymer materials were used to print the model of the mandible (Tab.1). Polylactic acid (PLA) was purchased from Prusa Research (Czech Republic). Polycarbonate (PC), PC-ISO, was provided by Stratasys (USA, Israel). Powdered polyamide 11 (PA11), Precimid 1170, was supplied by Solveere (Poland). Liquid polyacrylic photo resins such as E-Partial (AR1), E-Denstone (AR2) and FullCure 830 VeroWhite (AR3) were obtained from Stratasys (USA, Israel).

Mandible model preparation

The model of the mandible was obtained in the process of reconstructing data from the Siemens Somatom Sensation Open 40 multislice tomograph. Digital Imaging and Communications in Medicine (DICOM) data was made available from the Provincial Clinical Hospital No. 1 Fryderyk Chopin in Rzeszów. Based on the prepared data, the value of 200 HU was selected as the value of the lower segmentation threshold. The process of extracting the

a)



b)



Fig. 1. Views of model printing and measurement process: a) model orientation in the Fortus 360-mc printer space, b) 3D Talyscan 150 profilometer

Table 2. Selected 3D print systems

AM technology	AM technology	3D Printer (Manufacturer)	3D printing parameters (selected parameters)
Material Extrusion	Fused Filament Fabrication (FFF)	Prusa MK3s (Prusa Research, Czech Republic)	Nozzle type: 0.25 mm nozzle Nozzle temperature: 210°C Heatbed temperature: 50°C Print speed: 200 mm/s Cooling fan speed: 100% Layer thickness: 0.1 mm
	Fused Deposition Modeling (FDM)	Fortus 360 –mc (Stratasys, USA, Israel)	Nozzle type: T10 Nozzle temperature: 260°C Build plate temperature: 110°C Printing speed: 200 mm/s Recommended environmental temperature: 70°C Layer thickness: 0.178 mm
Vat Polymerization	Digital Light Processing (DLP)	Perfactory Vida (Envisiontec, Germany)	Projector 1920×1080 pixel Wavelength: 390–420 nm. Temperature: 10°C–40°C Humidity: 30%–75% Ambient pressure: 700–1060 hPa Layer thickness: 0.1 mm
	Scan, Spin, and Selectively Photocure (3SP)	3Dent – 3SP (Envisiontec, Germany)	Projector: 1920×1200 pixels Native pixel size: 0.1 mm) Pixel size: 0.05 mm Layer thickness: 0.03 mm
Powder Bed Fusion	Selective Laser Sintering (SLS)	TMP Elite 3600 (Solveere, Poland)	CO ₂ Laser power: 80 W Build speed: 15 mm/h Laser spot: 0.3 mm Max scanning speed: 1500 mm/s Layer thickness: 0.12 mm
Material Jetting	Material Jetting (MJ)	Eden 260V (Stratasys, USA, Israel)	Wavelength: 320–410 nm Humidity: 30%–70% Temperature: 18°–25°C Layer thickness: 0.016 mm

mandible from the entire data volume was carried out on it. The region growing method was used in the segmentation process, and the isosurface method was used to visualize the spatial model of the mandible. Then, the finished model of the mandible was saved to the STL format.

During the production of the models, the 3D printers parameters were optimized in order to obtain the lowest layer thickness (e.g. nozzle type, projector resolution or CO₂ laser power) (Tab.2).

Additionally, each model was vertically oriented in the working space of the machines during the printing

process (Fig.1a). The aim of this procedure was to create a polymer model in such a way so that its lateral surface would be most accurately reproduced and consistent with the origin model.

Methods

Measurements of the surface geometric structure of the model side part were carried out using a 3D Talyscan 150 contact profilometer by Tylor Hobson (Fig.1b) with a tip with a rounding radius of 2 μm and a cone angle of 60°.

Table 3. The obtained roughness parameters

Parameter [μm]	PLA	PC	AR1	AR2	PA11	AR3
S _q	6.40	7.34	1.78	2.82	9.58	6.29
S _p	11.86	10.04	13.11	8.15	35.19	20.19
S _v	19.71	25.50	7.92	15.53	32.81	20.54
S _t	31.58	35.54	21.04	23.68	68.00	40.73
S _{10z}	28.41	32.89	17.46	20.15	59.73	37.60
S _a	5.26	6.18	1.32	2.23	7.82	5.08

S_q – root mean square height, S_p – maximum peak height, S_v – maximum pit height, S_t – maximum height, S_{10z} – ten-point, S_a – arithmetical mean height

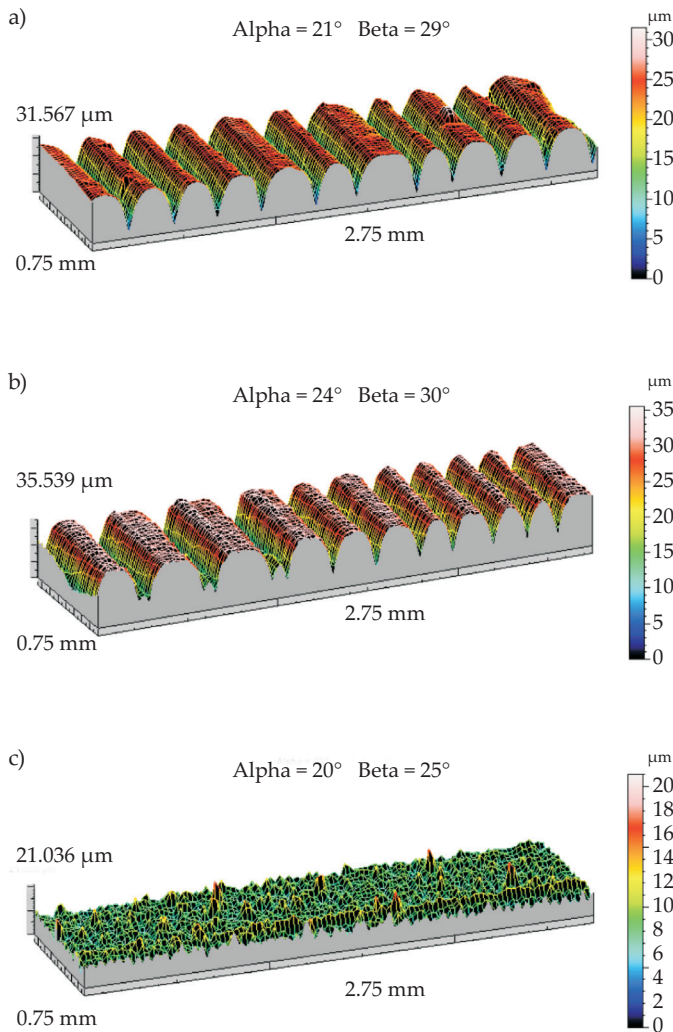


Fig. 2. 3D visualization of surface roughness of tested samples for materials: a) PLA (Prusa MK3s), b) PC (Fortus 360 – mc), c) AR1 (Perfactory Vida)

In the process of assessing the models surface roughness, the sampling step in the X and Y axes was set to the minimum value, equal to 5 μm . A single measured area was 3 \times 1 mm. During the measurement, the lowest available measurement speed of 2000 $\mu\text{m/s}$ was used. Based on the analyzed area, the average measuring range of the head was selected – 392 $\mu\text{m}/58\,978$ digits. During the measurement of one profile, the head was not raised before taking the next one. This procedure allowed to avoid introducing unnecessary oscillations during the measurement. In the process of determining the surface roughness of the tested models, the filtration process was carried out, which firstly involved removing the obtained shape deviations using the 3rd order polynomial method. Then, in order to separate the long-wave components, a profile filter $\lambda_c = 0.8$ mm was used, which marks the transition from roughness to waviness. The determination of the length of the sampling and measuring sections was developed in accordance with ISO 4288 [20] for periodic roughness profiles. As a result, the roughness parameters

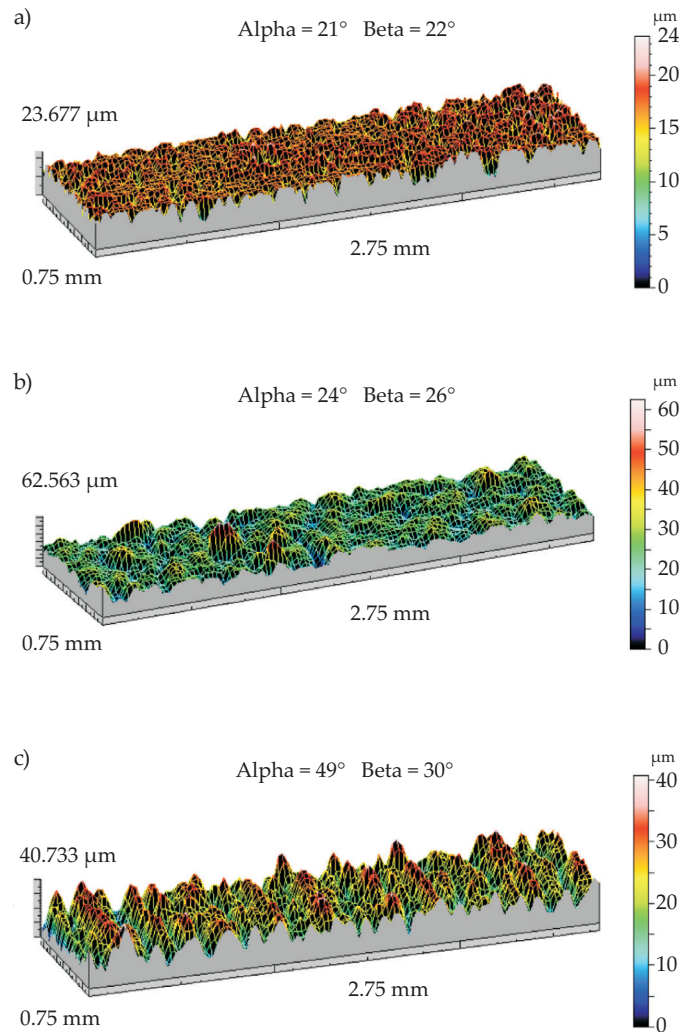


Fig. 3. 3D visualization of surface roughness of tested samples for materials: a) AR2 (3Dent – 3SP), b) PA11 (TMP Elite 3600), c) AR3 (Eden 260V)

were obtained (Tab. 3) along with a three-dimensional visualization of the examined area (Fig.2, Fig.3).

RESULTS AND DISCUSSION

The top layer of the material has a great influence on the properties of polymers made products, metals and ceramics. In the case of implants, the living organism reacts to the biomaterial by interacting with its surface layer [21]. Surface with a roughness coefficient of S_a about 4 μm is well tolerated by cells [22, 23]. Most of the implants have surfaces with $S_a = 1\text{--}2$ μm [24,25]. In the case of the polymeric materials presented in the work, some of them show biocompatibility. Especially it concerns PLA, PC and AR1 materials. In the case of models made with FFF and FDM techniques, a layered structure of surface roughness can be observed (Fig. 2a and Fig. 2b). The S_q values, which determine the standard deviation of the roughness for both methods, are very similar. However, the values obtained ($S_q = 6.4$ μm for PLA and

$S_q = 7.34 \mu\text{m}$ for PC) are much higher than for the Vat Polymerization techniques, which is related to a different process of creating a layered model. Additionally, when comparing the parameters S_v , the difference between both methods is almost $6 \mu\text{m}$. It may be related to the irregular application of successive layers of the model in the FDM technology. This aspect can be seen by comparing the three-dimensional visualizations of the surface roughness (Figs. 2a and 2b). As a result, it is possible to more accurately register the roughness in the pits between successive layers. The obtained values of the S_a parameter are similar (the difference for both methods is about $1 \mu\text{m}$). In order to achieve the recommended S_a value, it is necessary to perform further surface treatment, e.g. with a chemical method, after the model has been printed. Models made of PLA material are most often used in the orthopedic and dental industries [26], as well as in tissue engineering as biodegradable materials [27, 28]. The PC material is most often used in the production of surgical instruments. In the case of the AR1 material, the lowest value of the $S_a = 1.32 \mu\text{m}$ parameter can be observed among the analyzed materials. High precision and a smooth print surface are guaranteed in this case by DLP technology. Models made with this method are most often used in the dental industry as templates for correcting malocclusion [29]. In the case of acrylic resin AR2, a comparable value of the S_a parameter can be seen in relation to AR1. However, in the case of AR2, it is not biocompatible. The very good quality of the obtained model surface layer ($S_a = 2.23 \mu\text{m}$) brings benefits in terms of making accurate models used in reconstructive dentistry for the purpose of planning surgical procedures on them [30]. Despite the difference in layer thickness (DLP = 0.1 mm , 3SP = 0.03 mm), some similarities can be noticed in the obtained values of the amplitude parameters. However, in the case of the parameters S_p and S_v , there is some change. The surface roughness verified on the AR1 material is characterized by higher peaks above the average line than in the case of AR2 material. The situation is different for the S_v parameter. For the AR2 material, much larger pits below the mean line can be seen than for the AR1 material. The obtained values confirm the three-dimensional visualizations presented in Figures 2c and 3a. Currently, dental models made in the 3SP and DLP technology are slowly replacing traditional plaster models from the market. In the case of the AR3 material, the highest value of the $S_a = 5.08 \mu\text{m}$ parameter was obtained among all acrylic resins taken into account in the presented studies. The obtained statistical values are also confirmed by the three-dimensional visualization of the surface shown in Figure 3c. The presented results could have been influenced by the applied material curing source, which is an ultraviolet lamp. In the case of the 3SP technique, this is done by the use of a laser, and in the case of DLP, a special projector. Taking into account the SLS technique, the PA11 material was used. Despite the fact that this material is not biocompat-

ible, it is widely used in the production of medical equipment [31]. The obtained value of the $S_a = 7.82 \mu\text{m}$ parameter could mainly be influenced by a different method of bonding the material to the previously discussed techniques and post-process treatment, which is usually carried out with the use of compressed air or additionally with a cleaning agent.

CONCLUSION

The variety of additive techniques enables the wide use of commercially available polymer materials used in the process of making anatomical structures models on the basis of data from computed tomography. The obtained dental models play an important role in various types of procedures and operations, where appropriate surface roughness is required from the surgical template or implant model. Polyacrylic photo resins marked in the article as AR1 and AR2 meet the expectations regarding the implant's surface roughness. The AR3 material can be taken into account to prepare demonstrative models for use in medicine. In the case of PLA, PC, and PA11 materials, it is necessary to carry out a further surface treatment process. Therefore, in the next planned research, it is necessary to carry out further microgeometry analyzes of anatomical structures models made of polymeric materials in order to adapt their surface layer to medical requirements.

REFERENCES

- [1] Gibson I., Rosen D.W., Stucker B.: "Additive Manufacturing Technologies". Springer, Cham, Switzerland 2021.
- [2] Thompson M.K., Moroni G., Vaneker T., Fadel G., Campbell R.I., Gibson I., Bernard A., Schulz J., Graf P., Ahujai B., et al.: *CIRP Ann.* **2016**, 65, 737, <https://doi.org/10.1016/j.cirp.2016.05.004>.
- [3] Khaliq M.H., Gomes R., Fernandes C., Nóbrega J., Carneiro O.S., Ferrás L.L.: *Rapid Prototyp. J.* **2017**, 23, 727, <https://doi.org/10.1108/rpj-02-2016-0027>.
- [4] Leal R., Barreiros F.M., Alves L., Romeiro F., Vasco J.C., Santos M., Marto C.: *Int. J. Adv. Manuf. Technol.* **2017**, 92, 1671. <https://doi.org/10.1007/s00170-017-0239-8>.
- [5] Rokicki P., Budzik G., Kubiak K., Dziubek T., Zaborniak M., Kozik B., Bernaczek J., Przeszlowski L., Nowotnik A.: *Aircr. Eng. Aerosp. Technol. Int. J.* **2016**, 88, 374. <https://doi.org/10.1108/aeat-01-2015-0018>.
- [6] Turek P., Budzik G., Oleksy M., Bulanda K.: *Polimery* **2020**, 65, 510. <https://doi.org/10.14314/polimery.2020.7.2>.
- [7] Tack P., Victor J., Gemmel P., Annemans L.: *Biomed. Eng. Online* **2016**, 15, 115. <https://doi.org/10.1186/s12938-016-0236-4>

- [8] Ciocca L., Mazzoni S., Fantini M., Persiani F., Baldissara P., Marchetti C., Scotti R.A.: *Med. Biol. Eng. Comput.* **2012**, 50, 743.
<https://doi.org/10.1007/s11517-012-0898-4>.
- [9] Kumar B.P., Venkatesh V., Kumar K.A., Yadav B.Y., & Mohan S.R.: *Journal of maxillofacial and oral surgery* **2016**, 15, 425.
<https://doi.org/10.1007/s12663-015-0766-5>
- [10] Turek P., Pakla P., Budzik G., Lewandowski B., Przeszłowski Ł., Dziubek T., Wolski S., Frańczak, J.: *J. Clin. Med.* **2021**, 10, 5525.
<https://doi.org/10.3390/jcm10235525>
- [11] Haffner M., Quinn A., Hsieh T.Y., Strong E.B., Steele T.: *Ann Otol Rhinol Laryngol.* **2018**, 127, 338.
<https://doi.org/10.1177/0003489418764987>
- [12] Favier V., Zemiti N., Mora O.C., Subsol G., Captier G., Lebrun R., Crampette L., Mondaine M., Gilles B.: *PLoS One* **2017**, 12, e0189486.
<https://doi.org/10.1371/journal.pone.0189486>.
- [13] Narayanan V., Narayanan P., Rajagopalan R., et al.: *Eur Arch Oto-RhinoLaryngology.* **2015**, 272, 753.
<https://doi.org/10.1007/s00405-014-3300-3>
- [14] Rose A.S., Kimbell J.S., Webster C.E., Harrysson O.L.A., Formeister E.J., Buchman C.A.: *Ann Otol Rhinol Laryngol.* **2015**, 124, 528.
<https://doi.org/10.1177/0003489415570937>
- [15] Cohen A., Laviv A., Berman P., Nashef R., Abu-Tair J.: *Oral Surg Oral Med Oral Pathol Oral Radiol Endodontol.* **2009**, 108, 661.
<https://doi.org/10.1016/j.tripleo.2009.05.023>.
- [16] Mori K., Yamamoto T., Nakao Y., Esaki T.: *Neurol Med Chir (Tokyo).* 2011, 51, 93
<https://doi.org/10.2176/nmc.0a2012-0295>
- [17] Mori K.: *Skull Base.* **2009**, 19, 333.
<https://doi.org/10.1055/s-0029-1224862>.
- [18] Cheneboux M., Lescanne E., Robier A., Kim S., Bakhos D.: *J Laryngol Otol.* **2014**, 128, 586.
<https://doi.org/10.1017/S0022215114001297>
- [19] Eltorai A.E.M., Nguyen E., Daniels A.H.: *Orthopedics* **2015**, 38, 684.
<https://doi.org/10.3928/01477447-20151016-05>.
- [20] ISO 4288: 2011: Geometrical products specifications (GPS) – Surface texture: Profile method rules and procedures for the assessment of surface texture.
- [21] Jemat A., Ghazali M.J., Razali M., Otsuka Y.: *BioMed research international* **2015**, 2015, 791725.
doi: 10.1155/2015/791725.
- [22] Qu Z., Rausch-Fan X., Wieland M., Matejka M., Schedle A.: *Journal of Biomedical Materials Research* **2007**, 82, 658.
<https://doi.org/10.1002/jbm.a.31023>
- [23] Le Guehennec L., Lopez-Heredia M.A., Enkel B., Weiss P., Amouriq Y., Layrolle P.: *Acta Biomaterialia* **2008**, 4, 535.
<https://doi.org/10.1016/j.actbio.2007.12.002>
- [24] Dank A., Aartman I.H., Wismeijer D., Tahmaseb A.: *International journal of implant dentistry* **2019**, 5, 1.
<https://doi.org/10.1186/s40729-019-0156-8>
- [25] Batak B., Çakmak G., Johnston W. M., Yilmaz B.: *The journal of prosthetic dentistry* **2021**, 126, 254.
<https://doi.org/10.1016/j.prosdent.2020.11.029>
- [26] DeStefano V., Khan S., Tabada, A.: *Engineered Regeneration* **2020**, 1, 76.
<https://doi.org/10.1016/j.engreg.2020.08.002>.
- [27] Bulanda K., Oleksy M., Oliwa R., Budzik G., Gontarz, M.: *Polimery* **2020**, 65, 557.
<https://doi.org/10.14314/polimery.2020.7.8>.
- [28] Bulanda K., Oleksy M., Oliwa R., Budzik G., Przeszłowski Ł., Mazurkow A.: *Polimery* **2020**, 65, 430.
<https://doi.org/10.14314/polimery.2020.6.2>.
- [29] Ye N., Wu T., Dong T., Yuan L., Fang B., Xia L.: *American Journal of Orthodontics and Dentofacial Orthopedics* **2019**, 155, 733.
<https://doi.org/10.1016/j.ajodo.2020.12.022>.
- [30] Mazzoli A.: *Medical & biological engineering & computing* **2013**, 51, 245.
<https://doi.org/10.1007/s11517-012-1001-x>
- [31] Daule, V.M.R.: *Journal of Dental & Allied Sciences* **2013**, 2, 57.
<https://doi.org/10.4103/2277-4696.159285>.

Received 21 I 2022.